Vibration Region Extraction Method of Bridge Based on Ground-Based MIMO Radar [1]

Xiang Cao [1,2]; Xiangfei Nie [1]; Yunkai Deng [3]; Zhengquan Hu [1]; Fei Xiang [1,2];

[1]*School of Electronic and Information Engineering, Chongqing Three Gorges University, Chongqing, 404000, China*
[2]*Beijing Institute of Technology Chongqing Innovation Centre, Chongqing, 401120, China*
[3]*School of Information and Electronics, Beijing Institute of Technology, Beijing, 100081, China*

Abstract

Ground-based multiple-input multiple-output (GB-MIMO) radar is suitable for vibration monitoring of all kinds of bridges because of its high accuracy, wide detection range and non-contact characteristics. It is necessary to select effective pixels with stable amplitude and regular phase to achieve accurate estimation of bridge vibration. In this paper, a new method for extracting vibration regions of bridges based on GB-MIMO radar is proposed. In the first step, the mask in image processing is combined with the average amplitude to extract the bridge pixels in the radar image and the circle fitting method is used to suppress the static clutter in the bridge pixel sequence. In the second step, the amplitude dispersion index is used to screen out the points with stable pixel amplitude. In the third step, the pixels with stable amplitude are divided into vibrational and non-vibrational regions by vibration similarity. Finally, the Welch method is used to analyze the phase spectrum of pixel sequence in the vibration region to estimate the vibration frequency. In order to verify the effectiveness of the proposed algorithm for bridge vibration detection, the measured data of a bridge in Chongqing is taken as an example to test the algorithm. The results show that the algorithm improves the effective detection rate of vibration region.

Keywords

GB-MIMO radar; vibration area; static echo suppression; Frequency estimation

1. Introduction

Various kinds of bridge structures are affected by dynamic loads such as moving vehicles, crowds and earthquake during long-term use which will lead to fatigue damage or premature aging of local bridge structures. If the damaged part of the bridge structure cannot be identified and repaired in time. Over time, aging will accelerate further. It will lead to the accumulation of systemic damage of the bridge structure and the attenuation of bridge resistance and even cause serious disasters such as collapse, which poses a great threat to social property and people. Therefore, the research on bridge health monitoring technology is of great significance to ensure the normal and safe operation of highway bridges [1-2]. Vibration monitoring is an important method to evaluate the stability of bridge structure. As an advanced non-contact sensor, real aperture radar has been widely used in structural health monitoring. Its data acquisition speed is in the sub-millisecond level [3], but it has no azimuth resolution ability. GB-MIMO radar has the ability of two-dimensional high-resolution imaging which can resolve the vibration target in different directions on the same range gate and provides an effective technical means for vibration measurement.

Since the measurement of vibration by GB-MIMO radar needs to process and analyze the differential interference phase sequence of pixels in time and frequency domain, the pixels of radar image affected by noise are not suitable for vibration measurement. In order to achieve accurate estimation of bridge

ICBASE2022@3rd International Conference on Big Data & Artificial Intelligence & Software Engineering, October 21-23, 2022, Guangzhou, China
Cycnus.cao@qq.com (Xiang Cao)

vibration, effective pixels with stable amplitude and continuous phase need to be selected. In 1999, amplitude dispersion index (ADI) was proposed to effectively screen out points with relatively stable amplitude in pixel time series [6]. In 2007, the double threshold method of amplitude intensity and amplitude deviation index was proposed to solve the problem of ignoring the strong scattering of the target by the amplitude deviation method alone [7]. In 2019, Tian *et al*. [8] proposed the vibration similarity index (VSI) according to the frequency angle of the vibration phase sequence to represent the similarity between the phase sequence signal of the detected pixel and the ideal sinusoidal signal. The pixels with continuous phase sequence are effectively screened but the stability of scattering characteristics isn't considered and the pixels with unstable amplitude are easily selected. This article combines the characteristics of vibration pixels and phase sequences. The combination of ADI and VSI is used to screen the effective pixels of bridge vibration.

This paper is divided into five parts. The first part introduces the research background and content of this paper. The second part analyzes the vibration measurement principle of GB-MIMO radar. The third part describes the experimental methods. The fourth part discusses the test results of Chongqing Bridge. The fifth part is the summary of this paper.

2. Vibration measurement principle of GB-MIMO radar

The realization of vibration target localization by GB-MIMO radar mainly depends on the two-dimensional high-resolution capability of GB-MIMO radar. A series of two-dimensional high resolution radar images are generated by imaging the received signals [9-10]. The imaging results in an imaging unit can be expressed as

$$I(m,n)=\left|I(m,n)\right|e^{\mathrm{j}\frac{4\pi}{\lambda}R} \tag{1}$$

Where, $I(m,n)$ represents the imaging result after focusing at the position of grid (m,n). $\left|I(m,n)\right|$ is the amplitude of the imaging result. R is the radial distance between the scatterer of (m,n) and the radar.

According to equation (1), the phase of the imaging result of each pixel contains the distance information between the scatterer and radar in the scene corresponding to the pixel. For the vibration target in the scene, the phase of the imaging result will show a certain periodicity along with the vibration, so the phase curve of the multi-frame imaging result can be used for vibration analysis. After extracting the signal of the same imaging unit from multiple consecutive imaging results, the signal sequence of a vibrating object can be expressed as

$$I_{(m,n)}(k)=\left|I_{(m,n)}(k)\right|e^{\mathrm{j}\frac{4\pi}{\lambda}R_{vib}}e^{\mathrm{j}\frac{4\pi}{\lambda}A_{vib}\sin(2\pi f_{vib}k\Delta t)} \tag{2}$$

Where, $I_{(m,n)}(k)$ is the signal of imaging unit (m,n) in the k th imaging results. R_{vib} is the radial distance from the vibration center to the center of radar aperture. Δt is the time for collecting imaging data of an image. A_{vib} and f_{vib} represent the vibration amplitude and frequency of the vibrating object, respectively.

3. The proposed method

This paper is mainly divided into three parts: preprocessing, bridge vibration pixel extraction and frequency estimation. Firstly, the radar image is preprocessed to extract the target region and suppress the static echo of the vibration signal. Secondly, the vibration pixels of the bridge deck were screened by combining ADI and VSI. Finally, the frequency of the selected pixel sequence is estimated. The flow of the proposed method is shown in Fig. 1.

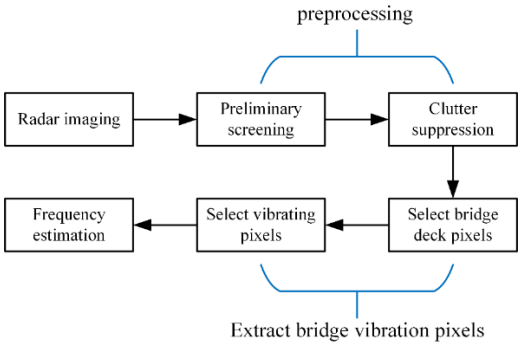

Fig. 1 Flow chart of bridge vibration region extraction

3.1. Preprocessing

The purpose of preprocessing is to extract target region from radar image region and suppress clutter. The first step is to extract the target region by using the mask in image segmentation according to the observed scene image. The second step is based on the strong scattering characteristics of the target echo signal, which is characterized by high energy and large amplitude of the echo signal. The average amplitude threshold method is used to detect the target region. The pixel with high amplitude is selected as the target candidate point by setting an appropriate threshold. The expression is as follows:

$$\overline{A}=20*\log_{10}\left(\frac{1}{K}\sum_{k=1}^{K}A_k\right),\quad k=1,2,\cdots,K \tag{3}$$

Where, A_k is the amplitude value of a pixel in the *kth* radar image. According to experience, the threshold can be set to -10dB [13].

Finally, according to the characteristics that the stationary target echo does not change with time while the vibration echo phase changes periodically with time, the circular fitting method [11] is used to suppress the stationary clutter of the target candidate pixel sequence.

3.2. Select bridge deck pixels

After preprocessing, the approximate range of bridge pixels is filtered out. Because the bridge is an artificial structure the surface is relatively smooth. The scattering intensity of each structure location is inconsistent and unpredictable. So, it is necessary to determine the pixels with high SNR when selecting the effective pixels. ADI is based on the statistical characteristics of pixel amplitude on the time series to select the point of amplitude stability. For a pixel with a high SNR, the noise level of its phase is equivalent to the amplitude dispersion index [6]. Therefore, the ADI method can effectively screen out the pixels with stable bridge amplitude by setting an appropriate threshold. The expression is as follows:

$$D_A=\frac{\sigma_A}{m_A} \tag{4}$$

In equation (3), σ_A and m_A are the amplitude standard deviation and amplitude average value of N radar images in the temporal dimension. D_A is the dispersion index. Empirically, the threshold can be set to 0.15 [12].

3.3. Select vibrating pixels

The bridge amplitude stable pixels selected by ADI can be directly used for deformation monitoring because the bridge deforms very slowly. In order to realize vibration monitoring of bridge, it is necessary to select pixels with regular phase. Vibration Similarity Index (VSI) [8-11] can represent the

Similarity between phase sequence signal and ideal sinusoidal signal. When the VSI is larger, the Vibration amplitude is larger. The expression is as follows:

$$\mathrm{VSI}=\frac{S_{\max}}{S_{\mathrm{mean}}} \tag{5}$$

Where, $S_{\max}$ and S_{mean} represent the peak amplitude of the spectrum after removing the DC component and the average amplitude of the whole spectrum, respectively. By setting an appropriate threshold $\mathrm{VSI}_{\mathrm{T}}$, the pixel meeting condition $\mathrm{VSI}>\mathrm{VSI}_{\mathrm{T}}$ is the vibration pixel. When choosing $\mathrm{VSI}_{\mathrm{T}}$, first determine the number of sampling points and the required detection probability. The detection rate is the probability that the highest value in the spectrum except the zero-frequency point corresponds to the vibration frequency. Then the requirement of SNR is obtained according to the required detection probability. Finally, we find the corresponding $\mathrm{VSI}_{\mathrm{T}}$ [8].

Finally, the common pixels of (4) and (5) are obtained. Since the vibration pixels of the structure are not isolated in the image domain, the isolated pixels are removed by the filtering operation in binary morphology.

3.4. Frequency estimation

As shown in Equation (2), the phase of the extracted signal includes the vibration of the vibrating object. Therefore, Welch method [16] can be used to estimate the vibration frequency according to the phase of the signal sequence. The expression is as follows:

$$P=\frac{1}{L}\sum_{i=1}^{L}\left|\sum_{n=1}^{N}x_i(n)\omega(n)\exp(-j\omega n)\right|^2 \tag{6}$$

Where x_i represents the ith data segment with N elements, L is the segment number, $\omega(n)$ is the window function. The position of the spectral peak corresponds to the estimated vibration frequency.

4. Bridge vibration experiment

4.1. Experimental information

A bridge in Chongqing was monitored by 16×16 GB-MIMO radar in the experiment. System parameters are shown in Table 1, and experimental scenes are shown in Fig 2

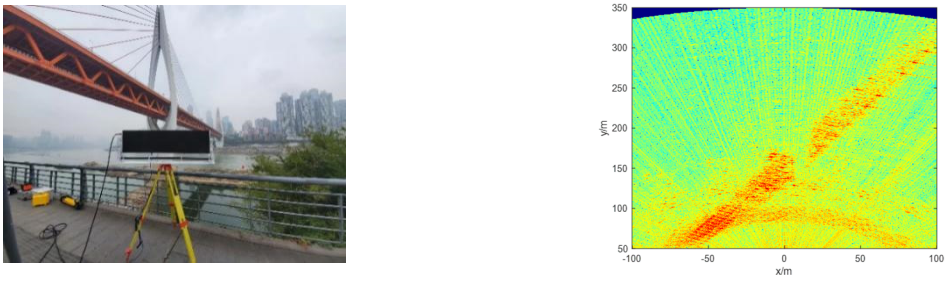

(a) Monitoring scene diagram (b) Imaging results

Fig. 2 Monitoring scene and MIMO radar imaging results

Table 1. GB-MIMO radar system parameters

Parameter	Value	Parameter	Value
Bandwidth	656 MHz	Central Frequency	16.2 GHz
Acquisition Frequency	47.84 Hz	Range Resolution	0.375 m
Azimuth Resolution	7.4 mrad	PRT	0.082 ms
Wavelength	0.0185 m	Measurement Range	50-500 m

4.2. Experimental results

A. Preprocessing: As mentioned in 3.1, Fig. 3 (a) plots the target area extracted by artificial mask in image processing. The entire bridge shape can be clearly seen from the target area. According to (3), the bridge pixels with large amplitude in the target area are screened out, as shown in Fig. 3 (b). Then the candidate pixels are suppressed by circle fitting. Firstly, the trajectory of the bridge pixel sequence is fitted to the complex plane to obtain the center of the circle and the center of the circle is moved back to the origin of coordinates, as shown in Fig. 3 (c). Fig. 3 (d) shows the pixel distribution after clutter suppression.

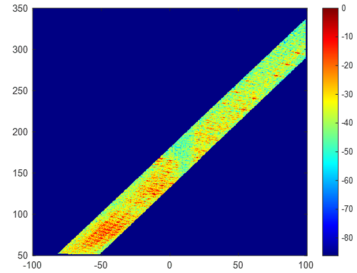

(a) Target area

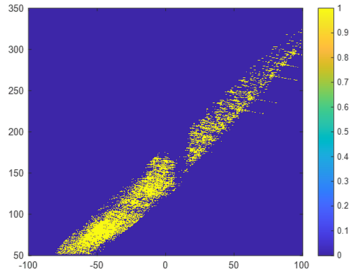

(b) Distribution of candidate pixels

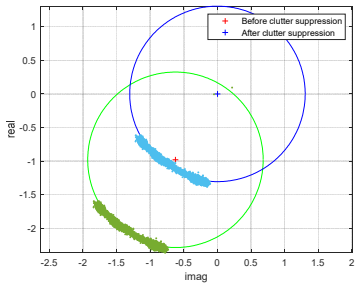

(c) Bridge pixel sequence trajectory

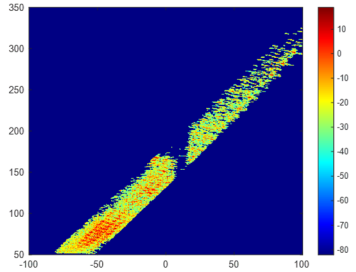

(d) Distribution after clutter suppression

Fig. 3 Data preprocess results

B. Select bridge deck pixels: The local graph of ADI value according to (4) is shown in Fig. 4 (a) after preprocessing. Some of the stronger amplitude pixels on the bridge have poorer ADI values due to dihedral Angle scattering and dwell. Fig.4 (b) shows the distribution of bridge deck pixels after screening by setting ADI threshold.

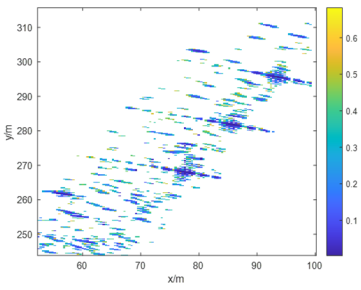

(a) Local graph of ADI value

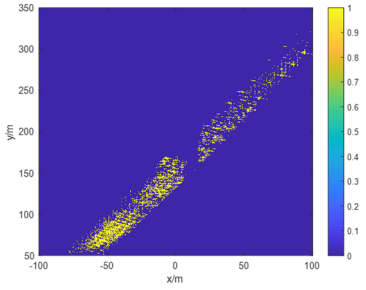

(b) Pixel distribution of bridge deck

Fig. 4 The rule of ADI

C. Select vibrating pixels: According to equation (5), the preprocessed pixel sequence is taken as the input to calculate the VSI then setting an appropriate threshold according to experience [8] to select the vibration pixels. Fig. 5 (a) shows the distribution of the vibration pixels. A total of 52302 vibrating pixels were selected. As the bridge body is a whole, its deformation in the same period should be regular [14]. The phase sequence of the selected pixels is used for deformation estimation [15]. Fig. 4 (b) shows the deformation curve of the selected pixels. The deformation of the bridge body is disorderly. This is because the selected vibration pixels of the bridge body include the vibration pixels outside the bridge

body. Therefore, it is necessary to screen the bridge structure pixels (pixels with stable amplitude) before screening the vibration pixels.

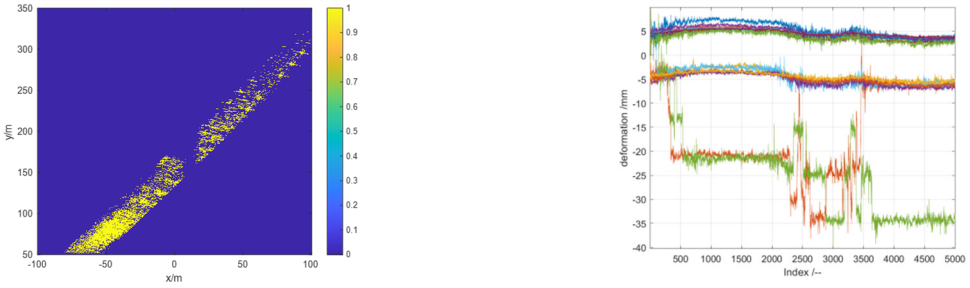

(a) Distribution of vibration pixel (b) Deformation curve

Fig. 5 VSI selection result

Finally, the pixels common to the bridge deck pixels and vibration pixels are defined as effective pixels, a total of 12587 pixels. Then, the isolated pixels are removed through binary morphology filtering operation, and a total of 12132 pixels are selected, as shown in Fig. 6 (a). Fig. 6 (b) shows the deformation curve of the effective pixel. The deformation changes of selected pixels are basically the same. Therefore, this method can effectively screen the vibrating pixels of the bridge deck.

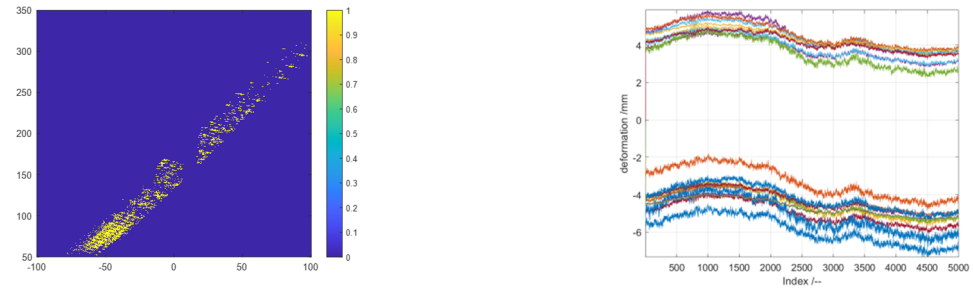

(a) Effective pixel distribution (b) Deformation curve

Fig. 6 Results of the proposed method selection

D. Frequency estimation: Fig. 7(a) depicts the phase curve of a vibrating pixel in the vibration area of the bridge. According to Section 3.4, the vibration frequency of the vibrating pixel is estimated to be 0.34Hz, as shown in Fig. 7(b). According to the data, the natural frequency of the first order vibration of long-span cable-stayed bridge is about 0.2~0.5Hz [17]. So, it is considered that the result is reliable.

(a) Vibration phase curve of vibrating pixels (b) Spectrum diagram of vibration phase curve

Fig. 7 The frequency spectrum

Finally, the vibration frequencies of the bridge vibration regions selected by the double threshold method and the bridge vibration regions selected by the VSI method are estimated respectively. Fig 8 (a) is the first-order frequency distribution of the proposed method and Fig 8 (b) is the first-order frequency distribution of the VSI method.

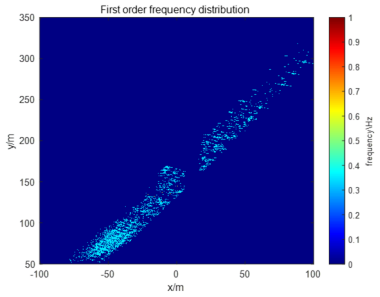

(a) First order vibration frequency distribution diagram (The proposed method)

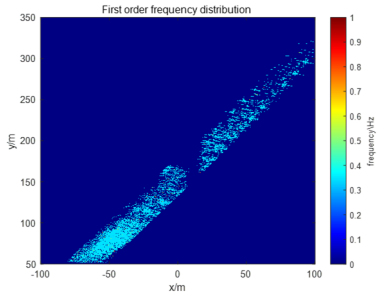

(b) First order vibration frequency distribution diagram (VSI method)

Fig.8 Vibration frequency distribution

In order to further compare the vibration region recognition effects of the two methods, the vibration frequencies in Fig. 8(a) and Fig. 8(b) were statistically analyzed. The results are shown in Table 2. The frequencies of pixels selected by the two methods are all concentrated at 0.34Hz. The pixels with a frequency of 0.34Hz selected by the proposed method accounted for 75.3% of the total selected structure pixels, which was larger than that of the VSI method. Therefore, the detection rate of bridge vibration region is higher with the proposed method.

Table 2 Estimation of vibration frequency

Method	Total points selected	Measured pixels	Vibration frequency	proportion
The proposed method	12132	9136	0.34 Hz	75.3%
VSI method	25512	18363	0.34 Hz	71.9%

5. Conclusion

In the bridge vibration measurement technology, in order to ensure the accuracy and reliability of the bridge vibration estimation, the bridge vibration region with stable amplitude and regular phase is selected. This article uses the stability characteristics of deck amplitude in time series and the energy distribution characteristics of vibration phase sequence spectrum. A method combining amplitude dispersion index and vibration similarity index is proposed, which can effectively improve the detection rate of bridge vibration region based on GB-MIMO radar. In the experiment, GB-MIMO radar is used to observe a bridge in Chongqing and obtain multiple radar image data continuously. The vibration region of radar image is selected by using the vibration similarity index method and the improved method. Finally, the frequency of selected vibration region is estimated by spectrum analysis principle. The experimental results show that the proposed method can effectively improve the detection rate of bridge vibration region.

6.Acknowledgments

This work was supported by the National Natural Science Foundation of China (619701037); Youth project of science and technology research program of Chongqing Education Commission of China. (Grant No. KJQN202101226).

7.References

[1] T. Pa, A. Ja, D. Ga, et al. "Remote Structural Health Monitoring System for Bridges", 2020 IEEE International Students' Conference on Electrical, Electronics and Computer Science (SCEECS), 2020, pp. 1-4.

[2] R. Li, T. Mo, J. Yang, et al. "Ontologies-Based Domain Knowledge Modeling and Heterogeneous Sensor Data Integration for Bridge Health Monitoring Systems", in IEEE Transactions on Industrial Informatics, 2021, vol. 17, no. 1, pp. 321-332.
[3] Y. Zhu, B. Xu, Z. Li, J. Hou, et al. "Monitoring Bridge Vibrations Based on GBSAR and Validation by High-Rate GPS Measurements", in IEEE Journal of Selected Topics in Applied Earth Observations and Remote Sensing, 2021, vol. 14, pp. 5572-5580.
[4] A. Zong. "Research on Radar MTI/MTD clutter suppression", Hubei University, 2012.
[5] K. Kulpa, B. Dawidowicz, L. Maslikowski, et al. "Single channel clutter cancelation in mobile PCL", 2018 22nd International Microwave and Radar Conference (MIKON), 2018, pp. 593-594.
[6] C. R. Farrar, T. W. Darling, A. Migliori, and W. E. Baker, “Microwave interferometers for non-contact vibration measurements on large struc-tures”, Mech. Syst. Signal Process. 1999, vol. 13, no. 2, pp. 241–253.
[7] X. Luo, D. Huang, G. Liu, et al. "Automatic detection of permanent scatterers in time serial differential radar interference", Journal of Southwest Jiaotong University, 2007, vol. 42, no. 4, pp: 414-418.
[8] W. Tian, Y. Li, C. Hu, et al. "Vibration Measurement Method for Artificial Structure Based on MIMO Imaging Radar", in IEEE Transactions on Aerospace and Electronic Systems, 2020, vol. 56, no. 1, pp. 748-760.
[9] A. Boag. "A fast multilevel domain decomposition algorithm for radarimaging", IEEE Trans. Antennas Propag, 2001, vol. 49, no. 4, pp: 666–671.
[10] H. Mei, Y. Li, W. Tian et al. "Weak Vibration Measurement Based on MIMO Imaging Radar System," 2018 China International SAR Symposium (CISS), 2018, pp: 1-5.
[11] P. Wang, Y. Xu, J. Xu, et al. "Study on removal method of static clutter from deformation monitoring signal of ground-based interference radar", Bulletin of Surveying and Imageping, 2014, no. 10, pp: 15-18+40.
[12] C. Hu, Y. Deng, W. Tian, and J. Wang. “A PS processing framework for long-term and real-time GB-SAR monitoring”, Int. J. Remote Sens. vol. 40, no. 16, pp. 6298–6314, Mar. 2019.
[13] M. Zhu. "High Precision Deformation Measurement Using Ground Based Synthetic Aperture Radar (GBSAR) Based on Dynamic Persistent Scatterer (PS) Technique", Beijing Institute of Technology, 2016.
[14] Z. Zhao, F. Jiang, G. Yin. "Brief Discussion on the Causes and Observation Methods of Bridge Deformation", Forest Engineering, 1999, no. 01, pp: 52-53.
[15] Y. Jia, Z. Gao, S. Liu, et al. "Application of FMCW MMW radar in dynamic deflection monitoring of high-speed railway bridge", Modern Electronics Technique, 2022, vol. 45, no. 15, pp: 15-19.
[16] W. Pan, L. Wang, Y. Song. "Recognition of Double- curvature Arch Bridge Natural Frequency Detection Signal Using Welch Power Spectrum Estimation", Industrial Control Computer, 2006, vol. 19, no. 11, pp: 22-23.
[17] B. Xiang, Y. Zhou. X. Chen. "Study on Dynamic Characteristics Monitoring System of Dongshuimen Yangtze River Bridge", Western Transportation Technology, 2015, no. 11, pp:46-50.